J|A|C|S
ARTICLES
Published on Web 06/25/2002

Growth and Structure Evolution of Novel Tin Oxide Diskettes

Zu Rong Dai, Zheng Wei Pan,† and Zhong L. Wang*

Contribution from the School of Materials Science and Engineering, Georgia Institute of Technology, Atlanta, Georgia 30332-0245

Received March 21, 2002

Abstract: The novel SnO diskettes have been synthesized by evaporating either SnO or SnO_2 powders at elevated temperature. Disregard the source material being SnO or SnO_2, the SnO diskettes are formed at a low-temperature region of 200−400 °C. Two types of diskette shapes have been identified: the solid-wheel shape with a drop center rim (type I) and the diskette with cone peak(s) and spiral steps (type II). The diskettes are determined to be tetragonal SnO structure (*P*4/*nmm*), with their flat surfaces being (001). The formation of the SnO diskettes is suggested to result from a solidification process. The structural evolution from SnO diskettes to SnO_2 diskettes has been investigated by oxidizing at different temperatures. The result shows that the phase transformation from SnO to SnO_2 occurs in two processes of decomposition and oxidization, and the decomposition process consists of two steps: first from SnO to Sn_3O_4 and then from Sn_3O_4 to SnO_2.

Introduction

Synthesis of nanomaterials with controlled morphology, size, chemical composition and crystal structure, and in large quantity is a key step toward nanotechnological applications. A number of nanomaterials in various geometrical morphologies have been produced, which include tubes,[1−8] cages,[9,10] cylindrical wires[11−18] and rods,[19−21] coaxial[22] and biaxial cables,[23] ribbons or belts,[24,25] and sheets.[26] The synthetic approaches include vapor-phase evaporation,[13,15−16,18−20,23−26] solution-phase growth,[11,21] sol−gel,[5,8] template-based method,[7,17] arc-discharge,[1−3,10] laser ablation,[12,14] and so forth.

SnO_2 is an n-type wide-band-gap semiconductor and a key functional material that has been extensively used for optoelectronic devices[27,28] and gas sensors detecting leakages of reducing gases such as H, H_2S, CO, and others.[29−34] Extensive work has been done on thin-film and nanocrystalline SnO_2.[35−38] Recently, stoichiometric SnO_2 nanobelts with a high quality crystalline rutile structure and uniform geometry have been successfully synthesized by simply evaporating a source material of either SnO_2 or SnO powders.[24,39] In addition to the synthesis of SnO_2 nanobelts, there have also been syntheses of SnO_2 nanowires,

* To whom correspondence should be addressed. Telephone: +1−404-894-8008. Fax: +1-404-894-9140. E-mail: zhong.wang@mse.gatech.edu.
† Current address: Chemical Sciences Division, Oak Ridge National Laboratory Oak Ridge, TN 37831-6201.

(1) Iijima, S. *Nature* **1991**, *354*, 56−58.
(2) Chopra, N. G.; Luyken, R. J.; Cherrey, K.; Crespi, V. H.; Cohen, M. L.; Louie, S. G.; Zettl, A. *Science* **1995**, *269*, 966−967.
(3) Bengu, E.; Marks, L. D. *Phys. Rev. Lett.* **2001**, *86*, 2385−2387.
(4) Rothschild, A.; Sloan, J.; Tenne, R. *J. Am. Chem. Soc.* **2000**, *122*, 5169−5179.
(5) Krumeich, F.; Muhr, H. J.; Niederberger, M.; Bieri, F.; Schnyder, B.; Nesper, R. *J. Am. Chem. Soc.* **1999**, *121*, 8324−8331.
(6) Remskar, M.; Mrzel, A.; Skraba, Z.; Jesih, A.; Ceh, M.; Demsar, J.; Stadelmann, P.; Levy, F.; Mihailovic, D. *Science* **2001**, *292*, 479−481.
(7) Satishkumar, B. C.; Govindaraj, A.; Vogel, E. M.; Basumallick, L.; Rao, C. N. R. *J. Mater. Res.* **1997**, *12*, 604−606.
(8) Adachi, M.; Harada, T.; Harada, M. *Langmuir* **1999**, *15*, 7097−7100.
(9) Tenne, R.; Homyonfer, M.; Feldman, Y.; *Chem. Mater.* **1998**, *10*, 3225−3238.
(10) Saito, Y.; Matsumoto, T. *Nature* **1998**, *392*, 237−237.
(11) Trentler, T. J.; Hickman, K. M.; Goel, S. C.; Viano, A. M.; Gibbons, P. C.; Buhro, W. E. *Science* **1995**, *270*, 1791−1794.
(12) Morales, A. M.; Lieber, C. M. *Science* **1998**, *279*, 208−211.
(13) Lee, S. T.; Wang, N.; Zhang, Y. F.; Tang, Y. H. *MRS Bull.* **1999**, *24*, 36−42.
(14) Duan, X. F.; Lieber, C. M. *Adv. Mater.* **2000**, *12*, 298−302.
(15) Chen, C. C.; Yeh, C. C.; Chen, C. H.; Yu, M. Y.; Liu, H. L.; Wu, J. J.; Chen, K. H.; Chen, L. C.; Peng, J. Y.; Chen, Y. F. *J. Am. Chem. Soc.* **2001**, *123*, 2791−2798.
(16) Huang, M. H.; Wu, Y. Y.; Feick, H.; Tran, N.; Weber, E.; Yang, P. D. *Adv. Mater.* **2001**, *13*, 113−116.
(17) Zheng, M. J.; Zhang, L. D.; Zhang, X. Y.; Zhang, J.; Li, G. H. *Chem. Phys. Lett.* **2001**, *334*, 298−302.
(18) Pan, Z. W.; Dai, Z. R.; Ma, C.; Wang, Z. L. *J. Am. Chem. Soc.* **2002**, *124*, 1817−1822.
(19) Dai, H. J.; Wong, E. W.; Lu Y. Z.; Fan S. S.; Lieber, C. M. *Nature* **1995**, *375*, 769−772.
(20) Yang, P. D.; Lieber, C. M. *J. Mater. Res.* **1997**, *12*, 2981−2996.
(21) Manna, L.; Scher, E. C.; Alivisatos, A. P. *J. Am. Chem. Soc.* **2000**, *122*, 12700−12706.
(22) Zhang, Y.; Suenaga, K.; Colliex, C.; Iijima, S. *Science* **1998**, *281*, 973−975.
(23) Wang, Z. L.; Dai, Z. R.; Gao, R. P.; Bai, Z. G., Gole, J. L. *Appl. Phys. Lett.* **2000**, *77*, 3349−3351.
(24) Pan, Z. W.; Dai, Z. R.; Wang, Z. L. *Science* **2001**, *291*, 1947−1950.
(25) Shi, W.; Peng, H.; Wang, N.; Li, C. P.; Xu, L.; Lee, C. S.; Kalish, R.; Lee, S. T. *J. Am. Chem. Soc.* **2001**, *123*, 11095−11096.
(26) Dai, Z. R.; Pan, Z. W.; Wang, Z. L. *J. Phys. Chem. B* **2002**, *106*, 902−904.
(27) Tatsuyama, C.; Ichimura, S. *Jpn. J. Appl. Phys.* **1976**, *15*, 843−847.
(28) Aoki, A.; Sasakura, H. *Jpn. J. Appl. Phys.* **1970**, *9*, 582−582.
(29) Watson, J. *Sens. Actuators* **1984**, *5*, 29−42.
(30) Yamazoe, N. *Sens. Actuators, B* **1991**, *5*, 7−19.
(31) Sberveglieri, G. *Sens. Actuators, B* **1992**, *6*, 239−247.
(32) Diéguez, A.; Romano-Rodríguez, A.; Morante, J. R.; Weimar, U.; Schweizer-Berberich, M. Göpel, W. *Sens. Actuators, B* **1996**, *31*, 1−8.
(33) Ansari, S. G.; Boroojerdian, P. B.; Sainkar, S. R.; Karekar, R. N.; Aiyer, R. C.; Kulkarni, S. K. *Thin Solid Films* **1997**, *295*, 271−276.
(34) Nayral, C.; Viala, E.; Collière, V.; Fau, P.; Senocq, F.; Maisonnat, A.; Chaudret, B. *Appl. Surf. Sci.* **2000**, *164*, 219−226.
(35) Schierbaum, K. D.; Weimar, U.; Göpel, W. *Sens. Actuators, B* **1992**, *7*, 709−716.
(36) Geistlinger, H. *Sens. Actuators, B* **1993**, *17*, 47−60.
(37) Bruno, L.; Pijolat, C.; Lalauze, R. *Sens. Actuators, B* **1994**, *18*, 195−199.
(38) Wang, D. Z.; Wen, S. L.; Chen, J. *Phys. Rev. B* **1994**, *49*, 14282−14285.
(39) Dai, Z. R.; Pan, Z. W.; Wang, Z. L. *Solid State Commun.* **2001**, *118*, 351−354.

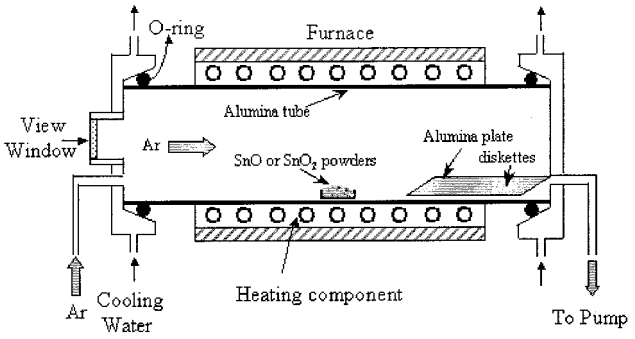

Figure 1. Schematic diagram of experimental apparatus for growth of tin oxide diskettes.

nanotubes, and nanoribbons composed of orthohombic-SnO_2 and tetragonal-SnO_2 phases.[40]

In this contribution, we report another novel structural form of tin oxide diskettes, synthesized by evaporating either SnO or SnO_2 powders. The as-synthesized tin oxide diskettes have the SnO stoichiometry and a tetragonal crystal structure. After annealing at certain temperature in an oxygen atmosphere, the SnO diskettes transform into rutile structured SnO_2. The formation of the SnO diskettes and the concrete process of the phase transformation from SnO to SnO_2 has been investigated and discussed.

Experimental Section

Experimental Apparatus and Material Growth. Thermal evaporation[13,24] was employed in the present investigation for synthesis of tin oxide materials. The experimental apparatus consists of a horizontal tube furnace (50 cm long), an alumina tube ($\Phi 4 \times 75$ cm), a rotary pump system, and a gas supply and control system. Figure 1 shows a schematic diagram of the furnace. A view window is set up at the left end of the alumina tube, by which it is possible to monitor the growth process. The right end of the alumina tube is connected to the rotary pump. Both ends are sealed by rubber O-rings. The ultimate vacuum for this configuration is $\sim 2 \times 10^{-3}$ Torr. The carrying gas comes in from the left end of the alumina tube and is pumped out at the right end.

Commercial (Alfa Aesor) SnO or SnO_2 powders ($\sim$4 g) with a purity of 99.9% (metals basis) were used as source material. The source material was loaded on an alumina boat and positioned at the center of the alumina tube. Inside the alumina tube, several alumina plates (60 $\times$ 10 mm) were placed downstream one-by-one, which acted as substrates for collecting growth products. After evacuating the alumina tube to $\sim 2 \times 10^{-3}$ Torr, thermal evaporation was conducted at 1070 °C for SnO powders or 1350 °C for SnO_2 powders for 2 h under the conditions of a pressure of 500−600 Torr and an Ar carrier gas of 50 sccm (standard cubic centimeters per minute). The tin oxide diskettes were collected in a $\sim$5-cm wide region downstream 30 cm away from the location of the source, where the temperature was in the range of 200−400 °C. It was noted that a similar product had been obtained at the same temperature zone whether the source material was SnO or SnO_2.

Material Characterization. The synthesized products were characterized by high-resolution field emission scanning electron microscope (SEM) (LEO 1530 FEG at 10 kV), field emission transmission electron microscope (TEM) (Hitachi HF-2000 FEG at 200 kV), high-resolution transmission electron microscope (HRTEM) (JEOL 4000EX at 400 kV), energy-dispersive X-ray spectroscope (EDS) attached to the SEM and TEM, and X-ray diffractometer (XRD) (Phillips PW 1800 at 40 kV and 30 mA).

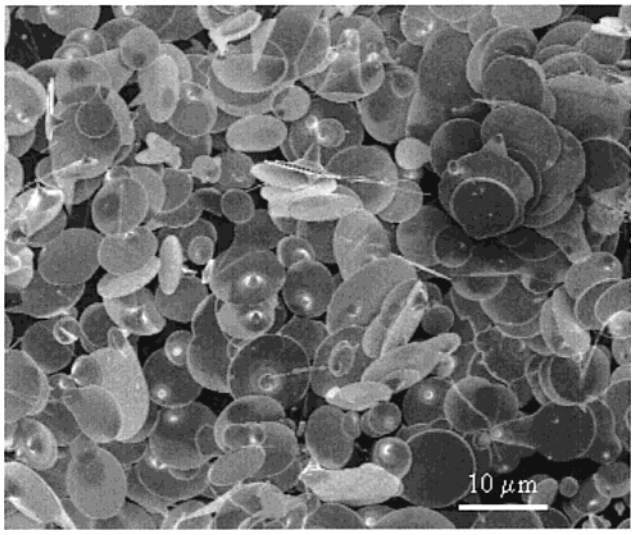

Figure 2. Typical SEM image of tin oxide diskettes.

Results and Discussion

Morphology of Tin Oxide Diskettes. Figure 2 is a SEM image showing the typical morphology of the product. The most striking result is that the product displays a diskette shape. The typical diameter of the diskettes in Figure 2 is 8−10 μm. The thickness of the diskettes is several tens to several hundreds nanometers, which varies with the dimension of corresponding diameter. The aspect ratio of diameter-to-thickness is about 15. Only Sn and oxygen elements are detected by EDS analysis, and the corresponding stoichiometry has been determined to be close to SnO. Some nanoscale tin oxide diskettes with diameter of 100−500 nm have also been observed at a place downstream farther from the source, where the temperature is relatively lower. This implies that the diameter of the tin oxide diskettes can be controlled by adjusting the temperature distribution inside the alumina tube. Tin oxide diskettes are always found together with SnO_2 nanobelts, and most of them suspend on the nanobelts. It is, however, very easy to separate the diskettes from the nanobelts by mechanical shaking, providing an opportunity that almost pure tin oxide diskettes are able to be extracted and investigated.

Two main types of SnO diskettes (types I and II) have been identified on the basis of morphology. The type I SnO diskettes (Figure 3) possess a uniform thickness and flat surfaces. A perfect circle contour is adopted by the type I SnO diskettes, of which diameters are larger than 1 μm (Figure 3a,b). The side view of a type I SnO diskette (Figure 3c) reveals that its geometrical shape is actually a solid wheel with a drop center rim. It appears that two wedged-rim diskettes stick together face-to-face. The including angle between two wedge planes is about 120°, as marked in the inset in Figure 3c. The diskette with the diameter less than 1 μm, however, displays a facet shape consisting of {110} and {100} crystal planes (Figure 3d). The details will be described and discussed in the following section. Some type I SnO diskettes have a tail extending from the edge (Figure 3e), which ends with a globule. EDS analysis indicates that the globule is Sn-rich.

(40) Dai, Z. R.; Gole, J. L.; Stout, J. D.; Wang, Z. L. *J. Phys. Chem. B* **2002**, *106*, 1274−1279.

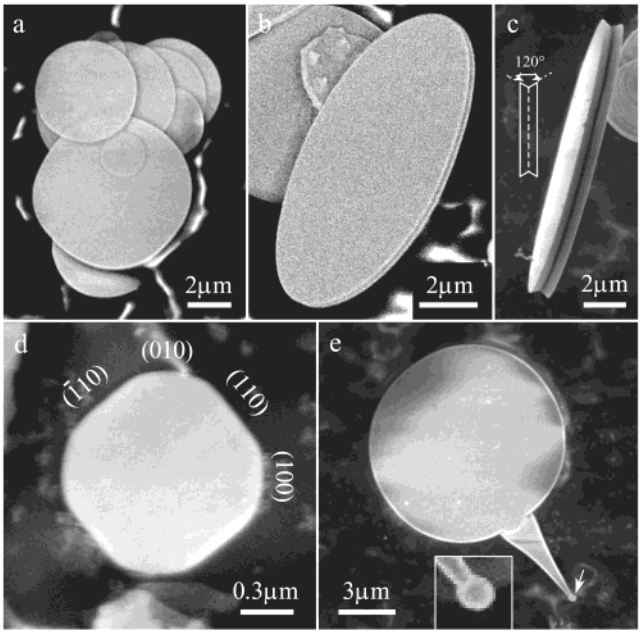

Figure 3. SEM images showing morphology of type I SnO diskettes. The inset in (c) is a schematic of side view shape of a type I SnO diskette. The inset in (e) is an enlarged image of the tip marked by an arrowhead, which indicates that the tip is a spherical ball.

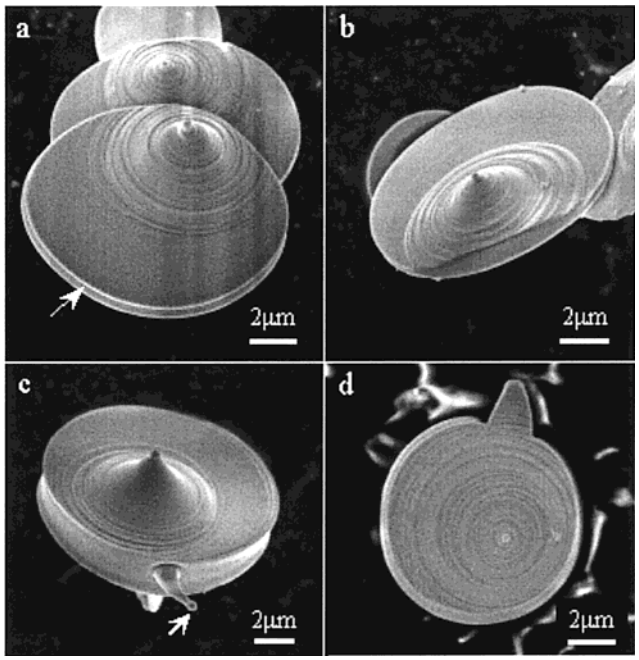

Figure 4. SEM images showing morphology of type II SnO diskettes with growth features of terraces and spiral steps.

Figure 4 shows several SEM images of the type II SnO diskettes, of which the top surfaces are not flat. Instead, terraces and spiral steps can be identified, resulting in the formation of a conelike peak on the top surface of the SnO diskettes. The center of the cone is not necessary to be located at the center of the diskette (Figure 4a−c). The apexes of cone peaks are globules that have been identified as Sn-rich, similar to the one associated with the tail of the type I SnO diskette (Figure 3e). The edge tail is also observed in the type II SnO diskettes, as indicated with an arrowhead in Figure 4c. The drop-center rim is also consistently observed with the type II SnO diskettes (e.g., as indicated by the arrowhead in Figure 4a).

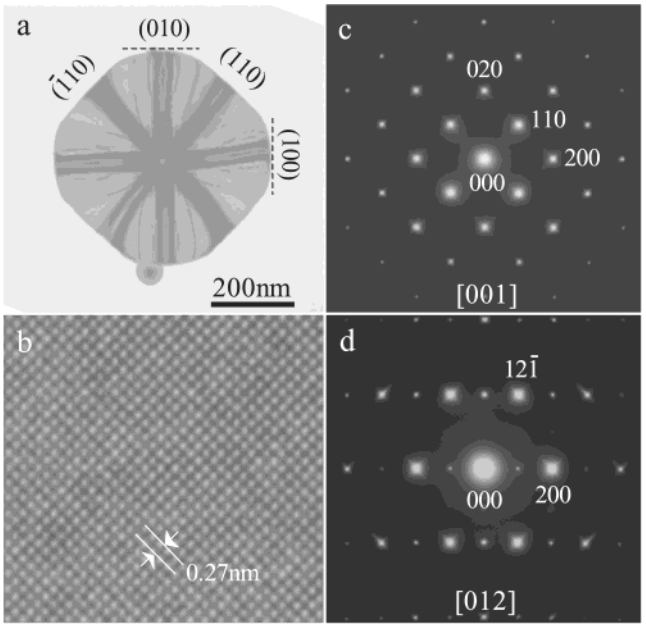

Figure 5. TEM image of an individual SnO diskette (a) and HRTEM image of the SnO diskette (b), which are recorded under the conditions of the electron beam parallel to [001] crystal direction. (c) and (d) Select area electron diffraction patterns taken from the same SnO diskette but different crystallographic orientations [001] and [012], respectively, where the indexes are given on the basis of the tetragonal SnO crystal structure with the space group *P*4/*nmm* and the lattice parameters: $a = 3.796$ Å and $c = 4.816$ Å.

Crystal Structure of SnO Diskettes. Tin monooxides mainly have three types of crystal structures: tetragonal SnO (α-SnO),[41] orthorhombic SnO,[42] and *β*-SnO.[43] To determine the crystal structure of the SnO diskettes, electron diffraction and X-ray diffraction techniques have been employed. A series of electron diffraction patterns have been recorded from the same SnO diskette while tilted along different crystallographic orientations. Analysis indicates that a SnO diskette is a single crystal and has the tetragonal SnO structure (*P*4/*nmm*, $a = 3.796$ Å and $c = 4.816$ Å),[41] of which the *a*- and *b*-axes are equivalent but not the *c*-axis. Two of the electron diffraction patterns are shown in Figure 5c,d that correspond to the [001] and [012] zone axes, respectively. A corresponding TEM image of the SnO diskette (Figure 5a) is taken under the condition of electron beam parallel to [001], the normal direction of the diskette. The regular pattern of the contrast over the SnO diskette in the bright field image displays the corresponding bending contour around the [001] zone axis.[44] HRTEM study (Figure 5b) indicates that the as-synthesized SnO diskette is singly crystalline and has high-quality crystallinity. It is evident that the SnO diskette (Figure 5a) displays a faceted shape with an octagon projection, which consists of two pairs of long straight parallel sides and two pairs of short arc sides. By combining the TEM image (Figure 5a) and its corresponding electron diffraction pattern (Figure 5c), it has been determined that the normal direction of the SnO diskette is [001] and the long straight sides are ±(110) and ±(1̄10) crystal planes. The central tangent planes of the short arc

(41) Moore, W. J.; Pauling, L. *J. Am. Chem. Soc.* **1941**, *63*, 1392−1394.
(42) Donaldson, J. D.; Moser, W.; Simpson, W. B. *Acta Crystallogr.* **1963**, *16*, A22-A22.
(43) Weiser, H. B.; Milligan, W. O. *J. Phys. Chem.* **1932**, *36*, 3039−3045.
(44) The diffraction contrast is produced as a result of a change in local diffracting conditions (e.g., deviation in excitation error). More details can be found in Hirsch, P. B.; Howie, A.; Nicholson, R. B.; Pashley, D. W.;Whelan, M. L. *Electron Microscopy of Thin Crystals*; Roberts E. Krieger Publishing: New York, 1977.

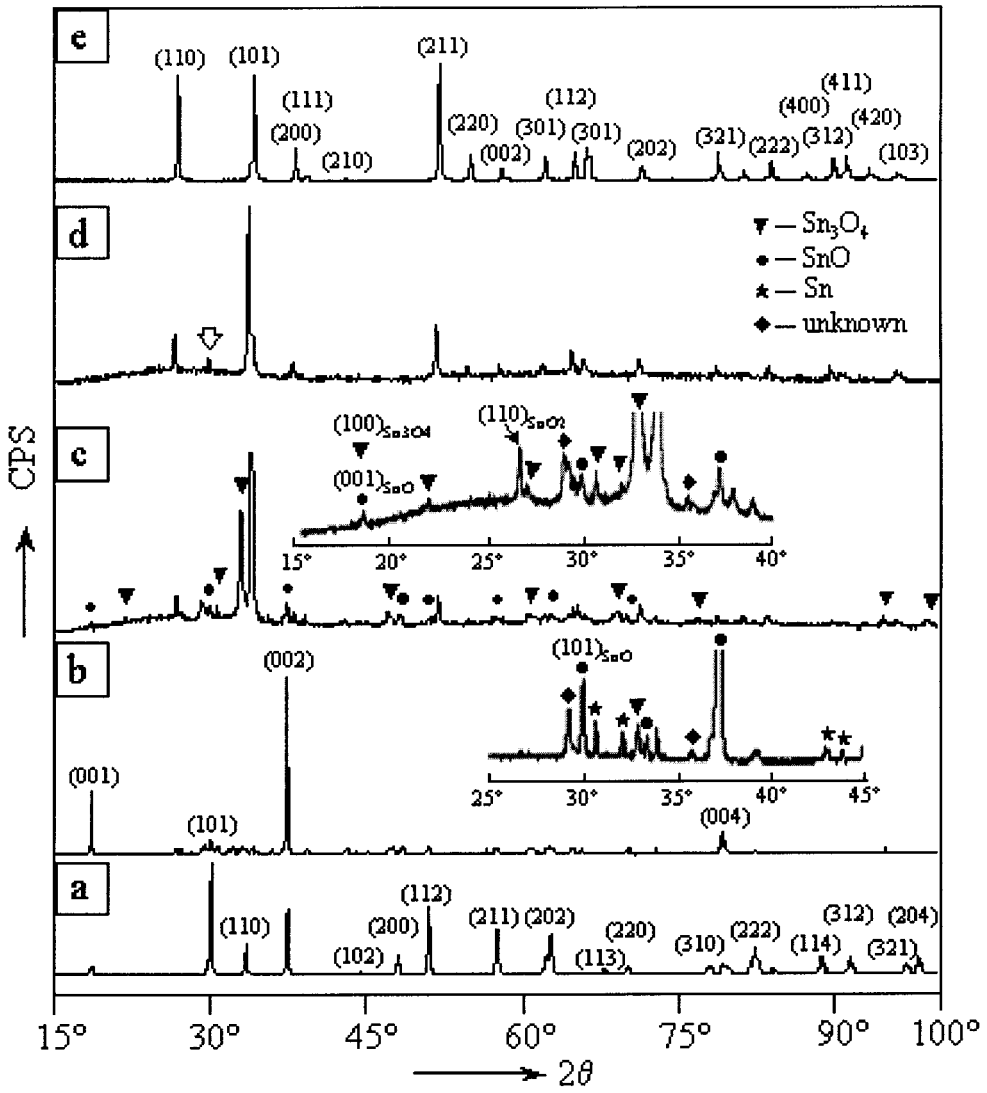

Figure 6. XRD spectra of standard SnO powders (a), as-synthesized SnO diskettes (b), SnO diskettes undergoing annealing at 500 °C for 2 h in oxygen atmosphere (c), SnO diskettes undergoing annealing at 700 °C for 2.5 h in oxygen atmosphere (d), and standard SnO_2 powders (e). The inset in (b) is an enlarged spectrum showing the details in the 2θ range of 25° to 45°, where the peaks marked by a (★) come from metal Sn and corresponding to its four main peaks (200), (101), (220), and (211), respectively. The peaks marked by a (●) in the spectrum (c) and inserted enlarged spectrum are contributed from SnO, the peaks marked by a (▼) from Sn_3O_4 and the peaks unmarked from SnO_2. The peaks marked by a (◆) come from some undetermined transitional phase or phases. The peak marked by an open arrowhead in (d) is likely from SnO and corresponding to (101) crystal plane.

sides are the ±(100) and ±(010) crystal planes of the tetragonal SnO. This indicates that at the initial stage the growth velocity of the SnO diskette along the [100] and [010] crystal directions is faster than that along the [110] and [$\bar{1}$10] crystal directions. As the dimension of the SnO diskette increases, the formation of a circle contour at the end is likely to lower the surface energy.

The XRD spectrum from the as-synthesized SnO diskettes (Figure 6b) shows a very strong feature of texture structure. When comparing this spectrum with the XRD spectrum acquired from standard tetragonal SnO powders (Figure 6a), the stronger peaks shown in Figure 6b are indexed to be (001), (002), and (004), indicating the formation of [001] texture structure in the SnO diskettes, which is consistent with the TEM observations and electron diffraction analyses. The XRD result supports that the as-synthesized SnO diskettes are of the tetragonal SnO crystal structure although some extra weak peaks occur in the XRD spectrum shown in the inset in Figure 6b, which are marked by symbols: (▼), (◆), and (★). The detailed interpretation of these weak peaks will be presented in the next section.

Phase Transformation from SnO to SnO_2. The tetragonal SnO is a thermodynamically unstable phase.[45] It might decompose into SnO_2 and Sn even at a relatively low temperature.[46] To obtain the stable rutile structured SnO_2, the as-synthesized SnO diskettes have been annealed in an oxygen atmosphere. Figure 6 shows five XRD spectra, among which the spectra shown in Figure 6a,e are taken from the standard SnO and SnO_2 powders, respectively, which are used as the reference spectra for the following analysis. The crystal structure of SnO powder is determined to be tetragonal ($P4/nmm$) with the lattice parameters: $a = 3.796$ Å and $c = 4.816$ Å.[41] The SnO_2 powders are of the rutile structure ($P4_2/mnm$) with the lattice parameters: $a = 4.737$ Å and $c = 3.185$ Å.[47] Most of the peaks in the XRD spectrum from as-synthesized SnO diskettes (Figure

(45) Humphrey, G. L.; O'Brien, C. J. *J. Am. Chem. Soc.* **1953**, *75*, 2805−2806.
(46) Brewer, L. *Chem. Rev.* **1953**, *52*, 1−75.
(47) Baur, W. H. *Acta Crystallogr.* **1956**, *9*, 515−520.

6b) fit with the tetragonal SnO, but some extra peaks are also identified, which come from some other minor phases. The inset in the Figure 6b is an enlarged spectrum in the range from 25° to 45°. Besides the peaks from SnO, as marked by (●), four characteristic peaks of metal Sn (β-Sn) ($I4_1/amd$, $a = 5.832$ Å and $c = 3.182$ Å)[48] are identified (marked by (★)), and are indexed to be the (200), (101), (220), and (211) reflections from Sn. The Sn peaks are likely from the globular tips that have been observed to be associated with the SnO diskettes. The peaks with no mark are from the remaining SnO_2 nanobelts because the SnO diskettes always coexist with the SnO_2 nanobelts which have been studied in detail elsewhere.[24,39] In fact, a few SnO_2 nanobelts can be identified in the SEM image shown in Figure 2.

The peak marked by a (▼) is likely from the Sn_3O_4 phase as discussed later. Two more weak peaks are still left, which are located at 28.6° and 35.8°, respectively, and are marked by (◆), which might come from some other intermediate phase(s). After annealing at 500 °C for 2 h in an oxygen atmosphere, the XRD spectrum (Figure 6c) has dramatically changed in comparison to the one shown in Figure 6b. The intensity of the SnO peaks marked by (●) significantly decreases, the rutile structured SnO_2 phase can be identified, and its diffraction peaks are unlabeled in the figure. In addition, some other peaks, as marked by triangle "▼", are clearly distinguished, which are determined to match the Sn_3O_4 phase that has a triclinic lattice structure with lattice parameters: $a = 4.86$ Å, $b = 5.88$ Å, $c = 8.20$ Å, $\alpha = 93.00°$, $\beta = 93.35°$, and $\gamma = 91.00°$.[49] The details can be found in the enlarged spectrum (inset in Figure 6c), where all main peaks of the Sn_3O_4 phase can be identified. At this stage, however, no peak of metal Sn can be found, indicating that the metal Sn identified originally in the as-synthesized sample has been oxidized during the annealing. Similar to those found in the enlarged spectrum inserted in Figure 6b, the two peaks located at 28.6° and 35.8°, respectively, are also identified in Figure 6c as marked by (◆). By increasing the annealing temperature to 700 °C, almost pure rutile structured SnO_2 is obtained (Figure 6d) in comparison to the standard spectrum from SnO_2 powders as given in Figure 6e. Only one extra peak with distinguishable intensity, as marked by an open arrowhead, has been found at the position of $2\theta = 29.8°$. The position is consistent with that of (101) peak of tetragonal SnO, indicating that a little amount of SnO might still remain. On the other hand, a certain texture structure still exists in the SnO_2 product since the intensity of (101) peak is abnormally strong compared with that of the SnO_2 powders' spectrum (Figure 6e).

It is, therefore, evident that the phase transformation from SnO to SnO_2 in an oxygen atmosphere is not a simple one-step process of oxidization but experiences some intermediate reactions. The solid-state SnO is thermodynamically unstable with respect to β-Sn and SnO_2.[50] The decomposition reaction of $2SnO(s) \rightarrow SnO_2(s) + Sn(l)$ was reported to occur starting at as low as 370 °C,[46] where the *s* and the *l* represent "solid state" and "liquid state", respectively. Some intermediate oxide phases such as Sn_3O_4,[49] Sn_2O_3,[51] and Sn_5O_6[52] were also reported

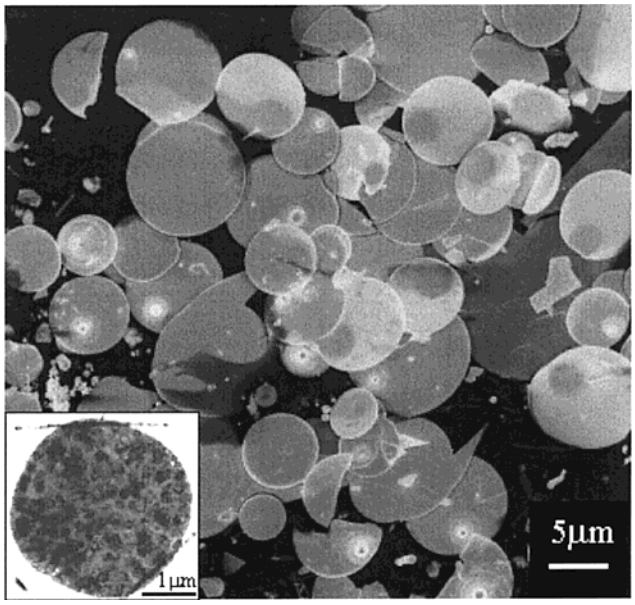

Figure 7. (a) SEM image of SnO_2 diskettes produced by oxidizing SnO diskettes in oxygen atmosphere at 700 °C for 2.5 h. (b) TEM image of an individual SnO_2 diskette.

to exist. Especially, the Sn_3O_4 was found to be formed by decomposition of SnO in a nitrogen atmosphere.[49] In the present study, however, the SnO diskettes are annealed in an oxygen atmosphere, and the Sn_3O_4 phase has also been clearly identified to coexist with SnO_2, but with the absence of Sn in the sample after annealing at 500 °C for 2 h. The Sn_3O_4 phase completely disappears after continually annealing the sample at 700 °C for 2.5 h. On the basis of these evidences, the following reactions are thought likely to be responsible for the $SnO \rightarrow SnO_2$ phase transformation in an oxygen atmosphere:

$$4SnO(s) \rightarrow Sn_3O_4(s) + Sn(l) \quad (1)$$

$$Sn_3O_4 \rightarrow 2SnO_2(s) + Sn(l) \quad (2)$$

$$Sn(l) + O_2 \rightarrow SnO_2(s) \quad (3)$$

Thus, the phase transformation from SnO to SnO_2 is conducted in two processes of decomposition and oxidization. The decomposition process consists of a two-step reaction 1 and 2, which is similar to that of the decomposition of SnO occurring in a nitrogen atmosphere.[49] The oxidization process 3 occurs simultaneously with the decomposition process and accelerates the decomposition reactions.

SEM observation (Figure 7) shows that most of the diskettes preserve their original shape after annealing at 700 °C for 2.5 h although the phase transformation from SnO to SnO_2 has been completed. This means that rutile structured SnO_2 diskettes can be obtained by annealing the SnO diskettes. A few diskettes are found to be broken possibly due to phase transformation-induced strain. The TEM study (inset) indicates that individual SnO_2 diskette is polycrystalline instead of the original single crystalline SnO, implying that the phase transformation from SnO to SnO_2 is not a simple one-step oxidizing process, therefore supporting the proposed two-step processes of decomposition and oxidization.

Formation of SnO Diskettes. In principle, the thermal evaporation technique is such a simple process that the source

(48) Deshpande, V. T.; Sirdeshmukh, D. B. *Acta Crystallogr.* **1961**, *14*, 355−356.
(49) Lawson, F. *Nature* **1967**, *215*, 955−956.
(50) Coughlin, J. P. *U.S. Bur. Mines Bull.* **1953**, *542*, 51−52.
(51) Murken, Von G.; Trömel, M. *Z. Anorg. Allg. Chem.* **1973**, *397*, 117−126.
(52) *JCPDS (International Center for Diffraction Data)* **1997**, 18−1386.

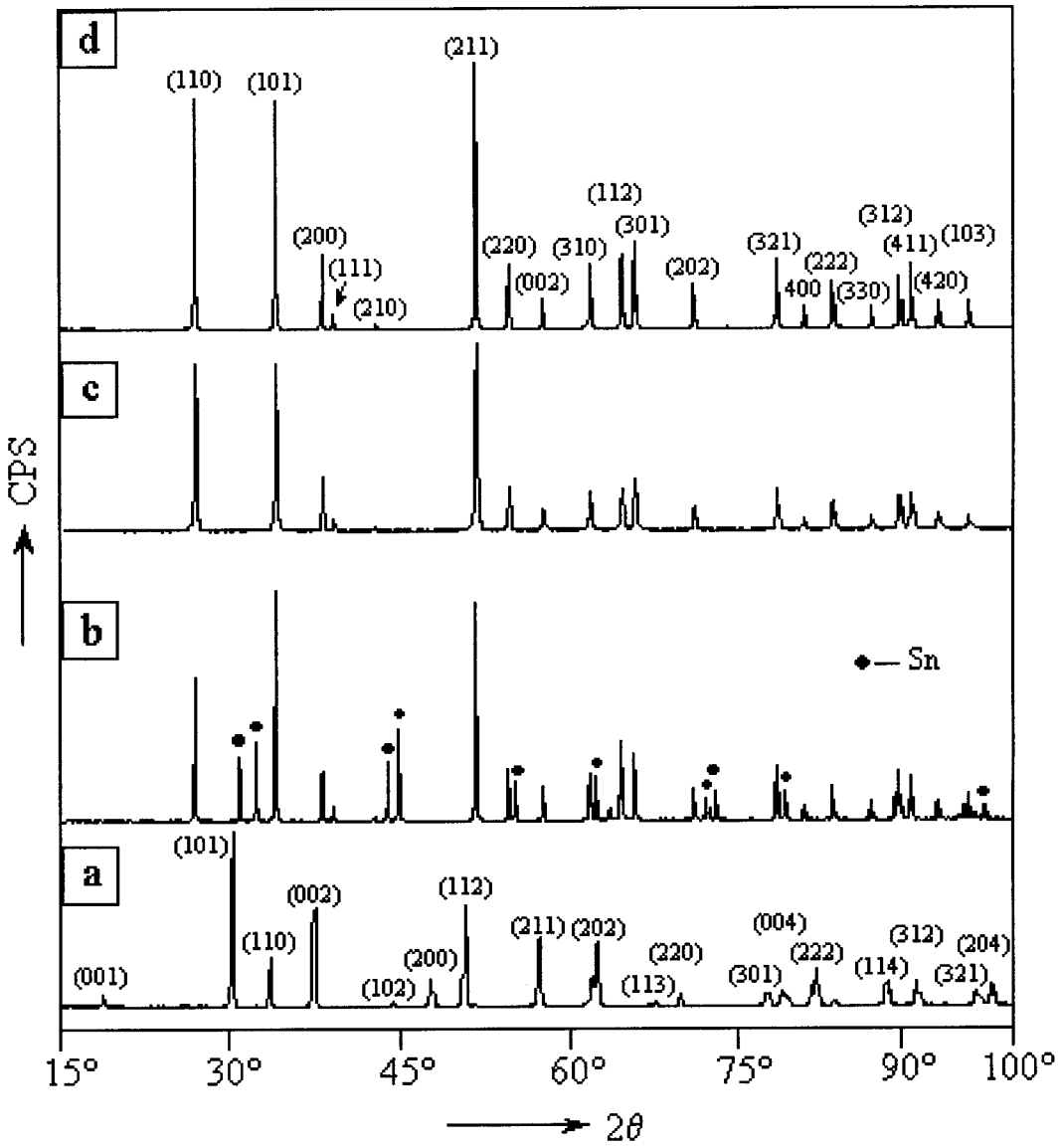

Figure 8. XRD spectra of original source material SnO powders (a) and the source after evaporating at 1070 °C for 2 h (b), where the peaks marked by (●) are contributed from metal Sn and other peaks from SnO_2. (c) XRD spectrum of original source material SnO_2. (d) XRD spectrum of the SnO_2 source evaporating at 1350 °C for 2.5 h.

material is evaporated by heating and then the resultant vapor phase(s) deposits at a certain conditions to form the product(s). The kinetic process included is, however, very complicated, depending on properties of the source material, the form of heating, the atmosphere and its movement state, the form of product collection, and the environment of product(s) growth including temperature, pressure, substrate, and so forth. For the compound source material, especially, some reaction(s) or decomposition often occurs, complicating the evaporation process. In the present study, although different source materials, either SnO powders or SnO_2 powders have been used, the same product of SnO diskettes is grown at the same temperature range of 200−400 °C, implying that the SnO diskettes are formed from the same precursor. It is, therefore, essential to study how the same precursor forms from the different source materials.

The SnO powder has a relatively lower melting point (1080 °C). It is, on one hand, easy to evaporate to form SnO vapors. On the other hand, solid-state SnO is an unstable phase in thermodynamics.[45] Decomposition may occur accompanied with evaporation. To provide more evidence for our discussion, the structure of the source material pre- and postevaporation has been investigated. Figure 8b shows an XRD spectrum from the source material of SnO powders after evaporating at 1070 °C for 2 h. By comparing with the XRD spectrum taken from original SnO powders (Figure 8a) and that from original SnO_2 powders (Figure 8c), it is evident that after the thermal evaporation, the SnO phase completely transforms to SnO_2 phase and metal Sn whose peaks are marked by (●), which proves that the decomposition of $SnO(s) \rightarrow SnO_2(s) + Sn(l)$ does occur. The occurrence of the decomposition decreases the rate of the SnO vaporization. In practice, controlling the oxygen concentration or partial pressure is a key to increasing the amount of SnO vapors.

As far as the SnO_2 powder source is concerned, it has been found that there are no structure changes after evaporating at 1350 °C for 2 h (Figure 8d) in comparison to the structure of the original SnO_2 powder (Figure 8c). It is, therefore, interesting to find out what has happened in the SnO_2 powder during the

heating and how it provides the precursor to produce the SnO diskettes. Thermodynamics analysis indicates that the reaction as follows will occur at high temperature.[53,55] where the *g*

$$SnO_2(s) \rightarrow SnO(g) + {}^1/_2O_2(g) \quad (4)$$

$$\Delta H_{298} = 134.9 \text{ kcal/mol}$$

$$\Delta G^0_{298} = 114.4 \text{ kcal/mol}$$

represents gas state and ΔH_{298} and ΔG^0_{298} denote standard enthalpy change and standard Gibbs free energy change, respectively. This means that the SnO vapors can be generated by thermal decomposition of SnO_2 at high temperature.

Although SnO(*g*) is relatively stable,[54] the following two reactions can happen spontaneously in thermodynamics during the process of lowering the temperature.[55]

$$SnO(g) + {}^1/_2O_2(g) \rightarrow SnO_2(s) \quad (5)$$

$$\Delta H_{298} = -134.9 \text{ kcal/mol}$$

$$\Delta G^0_{298} = -114.4 \text{ kcal/mol}$$

$$SnO(g) \rightarrow {}^1/_2SnO_2(s) + {}^1/_2Sn(l) \quad (6)$$

$$\Delta H_{298} = -65.6 \text{ kcal/mol}$$

$$\Delta G^0_{298} = -52.5 \text{ kcal/mol}$$

Reaction 5 actually is a process of reoxidization of the SnO vapors, and reaction 6 is a decomposition process of gas-state SnO. It is possible for both reactions to be responsible for SnO_2 products such as SnO_2 nanobelts. Another oxidized reaction might also occur in the system.[55]

$$Sn(l) + O_2 \rightarrow SnO_2(s) \quad (7)$$

$$\Delta H_{298} = -138.7 \text{ kcal/mol}$$

$$\Delta G^0_{298} = -123.9 \text{ kcal/mol}$$

Considering the standard Gibbs free energy change in both of oxidizing reactions 5 and 7, it is evident that oxygen more preferably reacts with liquid-state Sn than the SnO vapors. In the present study, the metal Sn has been clearly identified existing in the SnO source powders after evaporation (Figure 8b). This is an indication that the concentration of oxygen is limited in the present equipment system although a small leak is possible.[18] The metal Sn particles are also found coexisting with SnO_2 nanobelts at the high-temperature region (900−950 °C),[24,39] indicating the occurrence of the decomposition of SnO vapors. Thus, the decomposition of SnO vapors is likely the dominant process to be responsible for the formation of SnO_2 products in our system.

The gas-state SnO has a relatively lower condensation temperature. While a fraction of the SnO vapors decomposes to form SnO_2 nanobelts at high-temperature region (900−950 °C),[24,39] another fraction of SnO vapors may flow with the carrier gas to a lower-temperature region to form the SnO diskettes.

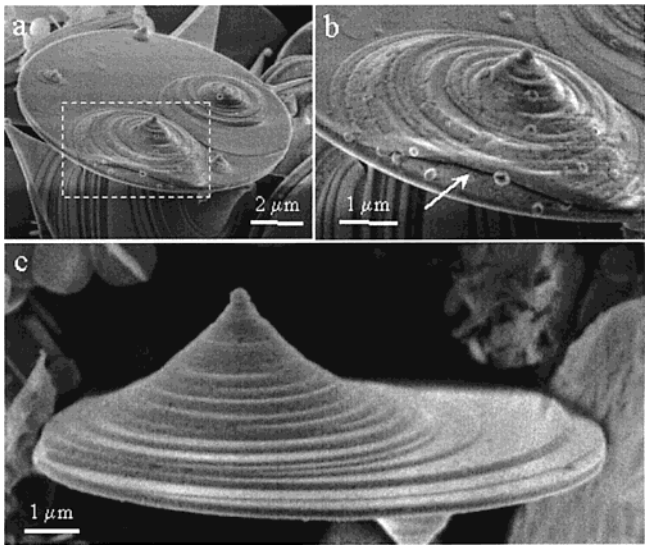

Figure 9. (a) SEM image of a SnO diskette with four conelike islands. (b) Enlarged image of the area within the frame shown in (a). (c) SEM image of an individual type II SnO diskette where the growth features of terraces and spiral steps are clearly seen.

Figure 9a shows an SEM image of a type II SnO diskette, where two larger and three smaller cone peaks exist. A feature of peeling off can be seen, as indicated by a white arrowhead in Figure 9b (an enlarged SEM image corresponding to the area within the box marked in Figure 9a). It is evident that the cone peaks form on the flat surface of type I SnO diskette, that is, a type II SnO diskette consists of a type I SnO diskette and cone peak(s). The growth of a cone peak is associated with spiral steps (Figure 9c).

Our experimental evidences indicate that the SnO diskettes are likely to grow following a solidification (liquid−solid) process. First, all of the SnO diskettes have a regular shape with a smooth circle contour and uniform chemical composition. Second, the Sn globules are found to be associated with the SnO diskettes. Third, the SnO diskettes are found to form at a relatively lower-temperature region (<400 °C), under which the SnO vapor phase is hard to maintain. During the growth of the SnO diskettes, as the SnO vapor moves with the carrier gas (Ar) into the low-temperature region, the SnO vapors may become super-cold liquid SnO droplets at first, provided that the flow of the carrier gas is very slow and the chamber pressure is relatively high, which are true in our case. Then the super-cold SnO droplets may condense onto either the alumina substrate or the surfaces of the SnO_2 nanobelts carried over by the carrier gas from the high-temperature region, resulting in the nucleation and growth by continuously receiving the incoming droplets. The formation of diskettes with a large (001) surface is possibly governed by crystal structure and surface energy. If the (001) surfaces of the crystallized SnO are constantly kept clean and the forming droplets can be kept constantly wet and cover the entire condensed (001) surface during growth, the type I SnO diskette will form. If some dirt or impurity is involved during the growth, around where the cone peak may form, this results in the formation of the type II SnO diskette. The spiral growth feature of the cone peak is

(53) Hoenig, C. L.; Searcy, A. W. *J. Am. Ceram. Soc.* **1966**, *49*, 128−134.
(54) Platteeuw, J. C.; Meyer, G. *Trans. Faraday Soc.* **1956**, *52*, 1066−1073.
(55) Kelley, K. K. *U.S. Bur. Mines Bull.* **1949**, *476*, 187−189.

similar to that of screw dislocation guided-growth process.[56] The globule located at the top of the cone peak is metal Sn originally. Since the liquid Sn has a certain dissolvability in liquid SnO,[57] as the solidification of the liquid SnO proceeds, the dissolved Sn will separate out from the SnO and solidify at last to form the globule because of its low melting point (232 °C).

The vapor−liquid−solid (VLS) growth[58] could be another possible mechanism responsible for the formation of the cone peaks and tails due to the catalytic effect of the Sn droplets, which leads to the deposition of SnO vapor onto the surface and formation of the spiral structure. The requirements of availability of the vapor phase in the growth region and long-range diffusion of atoms on the surface (especially for the cone peak growth) may, however, not be met under the lower temperature of <400 °C in a practical experiment. Of course, more experimental data are needed to clarify this situation.

Conclusions

Tin oxide has been found to exhibit nanostructures of belts/ribbons, wires, and tubes. In this work, a novel structure form of a tin oxide diskette is reported. The tin oxide diskettes have been synthesized by evaporating either SnO or SnO_2 powders at elevated temperature. Without regard for the source material being SnO or SnO_2, the same type of SnO diskette is formed at a low-temperature region of 200−400 °C, indicating that the growth is produced by the same precursor. Two types of diskette morphologies have been observed, the solid-wheel shape with a drop center rim (type I), and the diskette with cone peak and spiral steps (type II). Electron microscopy and X-ray diffraction show that the as-synthesized diskettes are tetragonal SnO structures (*P*4/*nmm*), with their flat surfaces being (001). For the case of SnO being the source material, the formation of SnO diskettes is within expectation. For the case of SnO_2 being the source material, the formation of SnO diskettes is proposed to result from a decomposition process of $SnO_2 \rightarrow SnO + {}^1/_2O_2$ at high temperature. Since the growth of the diskettes occurs at a lower-temperature region of 200−400 °C, the growth of the SnO diskettes is proposed to result from a solidification process. The structural evolution from SnO diskettes to SnO_2 diskettes has been investigated by oxidizing the sample at different temperatures. X-ray diffraction shows that the transformation occurs in two processes involving decomposition and oxidization and that the decomposition process consists of two-steps: first from SnO to Sn_3O_4 and then from Sn_3O_4 to SnO_2.

Acknowledgment. Thanks are due to the financial support of the U.S. NSF Grant DMR-9733160, and to the Georgia Tech Electron Microscopy Center for providing the research facility.

JA026262D

(56) Frank F. C. *Discuss. Faraday Soc.* **1949**, *5*, 48−54.
(57) *Binary Alloy Phase Diagrams*, 2nd ed.; Massalski, T., Okamoto, H., Subramanian, P. R., Kacprzak, L., Eds.; American Society for Metals: Metals Park, OH, 1990; pp 2919−2920.
(58) Wagner, R. S.; Ellis, W. C. *Appl. Phys. Lett.* **1964**, *4*, 89−90.